J. Membrane Biol. 129, 59–69 (1992)

The Journal of
Membrane Biology

Sarcolemmal Calcium Binding Sites in Heart: II. Mathematical Model for Diffusion of Calcium Released from the Sarcoplasmic Reticulum into the Diadic Region

Arthur Peskoff†, Jan A. Post‡*, and Glenn A. Langer‡

†Departments of Biomathematics and Physiology, University of California at Los Angeles School of Medicine, Los Angeles, California 90024-1766, and ‡Cardiovascular Research Laboratory, Departments of Physiology and Medicine, University of California at Los Angeles School of Medicine, Los Angeles, California 90024-1760

Summary. We present a model for predicting the temporal and spatial dependence of [Ca] in the cardiac subsarcolemmal diadic region (cleft), following Ca release from the "feet" of the sarcoplasmic reticulum. This region is modeled as a disc 10 nm thick, 430 nm in radius, with or without Ca binding sites and open at its periphery to the cytosol. [Ca] is computed for three diffusion coefficients (100, 20 and 4% of aqueous diffusion), following release of a 20-msec square pulse sufficient to produce 50% maximal contractile force, or repetitive release (400/min) of such pulses. Numerical solutions are obtained for the general diffusion/binding problem and analytic solutions for the case of no binding sites. For the middle value of diffusion coefficient, and in the absence of binding sites, [Ca] rises to ~1.5 mM in 20-msec and then falls to ~0.1 μM in < 3 msec. Adding binding sites reduces peak [Ca] to ~0.6 mM but prolongs its decline, requiring ~200 msec to reach 20 μM. For repetitive release [Ca] is > 100 μM for roughly half of each cycle. Two major implications of the predicted [Ca] are: (i) The effect of Ca binding sites on [Ca] will cause Ca efflux from the cleft via the Na-Ca exchanger (K_m(Ca) ≈ 20 μM) to continue at a significant level for > 200 msec. (ii) The time constant for inactivation of release from the "feet" must be much greater than for activation if Ca-induced Ca release is to continue for > 1–2 msec.

Key Words diffusion model · subsarcolemmal space · calcium diffusion · calcium exchange · calcium binding · excitation-contraction coupling

Introduction

In the preceding paper (Post & Langer, 1992) the sarcolemmal calcium (Ca) binding sites of the cardiac cell were further characterized. There are two classes of sites: K_d = 13 μM and 1.1 mM, with the low-affinity sites having 12 times the capacity of the high-affinity sites. It was shown that the low-affinity sites are phospholipid in nature and are located in the sarcolemmal cytoplasmic leaflet. The Ca concentration in cardiac cells has been observed to vary from a diastolic level of 0.1 μM to a systolic level of 5 μM. If the low-affinity sites were in an environment with such Ca concentrations, then the amount of Ca bound to the low-affinity sites would be very low. However, much higher Ca concentrations could exist in restricted compartments of the cell and go undetected by present techniques. A possible candidate for such a compartment would be the space ("cleft") between the cytoplasmic leaflet of the sarcolemma and the junctional sarcoplasmic reticulum (SR), into which, upon excitation, the Ca is released from the SR "feet" processes. Based upon data on SR Ca release, Ca diffusion, morphology of the cleft and sarcolemmal Ca binding sites, we constructed a mathematical model to calculate the Ca concentration in the cleft as a function of space and time.

The Ca concentration profile in the cleft is first calculated in the absence of binding sites. This is done for three values of the calcium diffusion coefficient: $D = 5 \times 10^{-6}$ cm^2/sec, representing the aqueous diffusion coefficient (Wang, 1953; Hodgkin & Keynes, 1957; Kushmerick & Podolsky, 1969; Nasi & Tillotson, 1985), and 20 and 4% of this value to span the range of diffusion coefficients reported within cells (Hodgkin & Keynes, 1957; Kushmerick & Podolsky, 1969; Nasi & Tillotson, 1985). Next, on the basis of previous work (Post et al., 1988; Post & Langer, 1992), we add the binding sites to the inner sarcolemmal leaflet with the density and with the K_d values measured. Their effect on the Ca concentration profile in the cleft is analyzed for the condition in which the sites are homogeneously distributed over

* *Present address:* Institute of Biomembranes, State University Utrecht, 3584 CH Utrecht, The Netherlands.

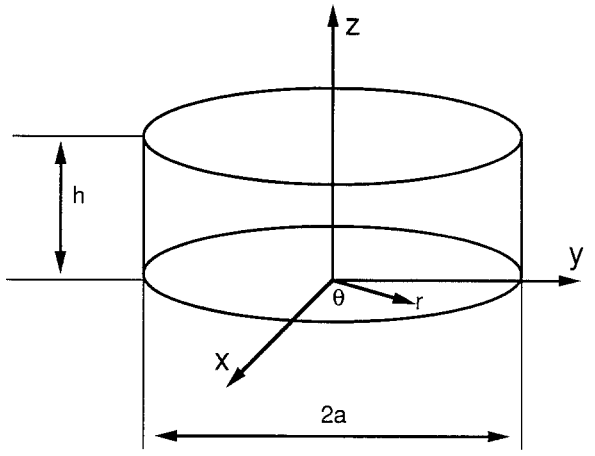

Fig. 1. Geometry of the model. The restricted space is modeled as a cylinder of height h and radius a. In a cylindrical coordinate system (r, θ, z), the surface of the SR cistern is at $z = 0$ and is a circle of radius $a = 430$ nm. The inner sarcolemmal surface facing it is at $z = h = 10$ nm. The cylinder is open to the cytosol at $r = a$.

the entire inner leaflet area. This is done with only the low-affinity (K_d = 1.1 mM) sites and with both low- and high-affinity (K_d = 1.3 μM) sites. We consider two time courses of Ca release. First, we consider a single square pulse of 20-msec duration, and then we consider a train of such pulses repeated every 150 msec to simulate beating.

The analysis demonstrates that the addition of sarcolemmal binding sites has a dramatic effect on the time dependence of the Ca concentration transient. With phospholipids containing the low-affinity sites homogeneously distributed, the high-affinity sites also present and $D = 10^{-6}$ cm^2/sec, the release of an amount of Ca at the "feet" sufficient to produce 50% maximal force results in a [Ca] averaged over the restricted space which reaches a peak value of > 0.6 mM and requires 200 msec to fall to 20 μM. If this profile represents the in vivo condition it would have significant physiological consequences for cellular Ca exchange.

The Model

Figure 1 illustrates the geometry of the "cleft" between the SR cistern and the inner sarcolemmal leaflet—the region which is spanned by the "feet." The surface of the cistern facing the sarcolemma is modeled as a circular disc of radius $r = a = 430$ nm (Page, 1978) in the plane at $z = 0$. The inner sarcolemmal surface is modeled as a plane a distance of 10 nm from the SR plane, the approximate height of the feet (Wagenknecht, 1989), located at $z = h = 10$ nm. The Ca released via the feet into this space upon excitation is the amount calculated by Fabiato (1983) to produce 50% maximum force, 8.8×10^{-20} mol/μm^3 cell water or 2.76×10^{-15} mol/cell (for a cell of 20 μm $\times$ 100 μm dimension). The diadic junctions or cleft regions are calculated (Page, 1978) at approximately 3.8×10^3/cell, and thus, the Ca released into each diadic region or cleft is 7.3×10^{-19} mol. We assume a release time of 20 msec (Feher & Fabiato, 1990) and since the precise form of the release is unknown we assume a square pulse with Ca release at the rate of $I = 3.65 \times 10^{-17}$ mol/sec. The release is assumed to occur uniformly throughout the volume of the space as well as uniformly in time, since the spatial distribution of the Ca release also is not known.

The outer boundary of the cleft at $r = a$ is assumed to be open to the general intracellular space where the concentration varies between a diastolic level of 10^{-4} mM and a systolic level as much as 50 times higher. In the model, we assume the concentration as $r = a$ is fixed at 10^{-4} mM. Taking into account the higher systolic level would raise the predicted [Ca] in the cleft. Its effect is not modeled because it would not significantly affect the predicted [Ca] if the concentration at $r = a$ never rose to levels comparable to the average value within the cleft. According to our results below, this appears to be the case.

Initially, we consider the steady-state diffusion problem in which the SR release occurs at a constant rate for all time. This is done to determine the maximum [Ca] that can be expected within the cleft from our model for the three values of the diffusion coefficient. Next we consider the transient problem without sarcolemmal binding sites. This shows the time required to reach maximum level after release commences and the time required to return to the diastolic level after release ceases. Both the steady-state problem and the transient problem without binding are solved analytically, the former in terms of a parabola, the latter in terms of an infinite sum of exponentials in time and zero-order Bessel functions in space.

We consider the transient problem with the two classes of the experimentally characterized binding sites following Michaelis-Menten relations. The resulting nonlinear diffusion equation is solved numerically by finite differences. Finally, we consider the response to repetitive excitation, with the SR release a train of square pulses.

In the present model we do not include the operation of Ca transport processes such as Na–Ca exchange and re-uptake of Ca by the SR. These are considered to be systems which, if juxtaposed to the cleft, would respond to the [Ca] profile modeled here. The addition of these systems to the present model will be approached in the future.

Steady-State Problem

In this section, we consider the steady-state problem. We assume the Ca release at a rate of $I = 3.65 \times 10^{-17}$ mol/sec has been flowing for a sufficient time so that the Ca distribution has reached a steady state.

We assume a uniform Ca current source s per unit volume of magnitude

$$s = I/\pi a^2 h. \tag{1}$$

Because $a = 43h \gg h$, variations in the z-direction can be neglected. Because of the symmetry of the problem, the Ca flux will be in the radial direction (dependent on r, but independent of θ and z). The radial Ca flux density J (mol/sec)/cm^2 at a distance r from the center of the cleft is

$$J = \pi r^2 hs/2\pi rh = Ir/2\pi a^2 h. \tag{2}$$

According to Fick's first law of diffusion, the Ca flux density is related to the Ca concentration by

$$J = -Ddc/dr \tag{3}$$

where $c(r)$ is the Ca concentration at radial distance r and D is the diffusion coefficient. Combining Eqs. (2) and (3) yields

$$dc/dr = -Ir/2\pi a^2 hD. \tag{4}$$

This may be integrated, using the boundary condition

$$c(a) = c_0 \tag{5}$$

to obtain

$$c(r) = c_0 + (I/4\pi Dh)(1 - r^2/a^2) \tag{6}$$

so that $c(r)$ has a parabolic distribution, with a peak value of $c_0 + I/4\pi Dh$ at the center of the cleft and a mean value of

$$c_m = \int_0^a c(r) \cdot 2\pi r dr/\pi a^2 = c_0 + I/8\pi Dh. \tag{7}$$

Notice that c_m, written in Eq. (7) in terms of the total current I per cleft, is independent of the cleft radius, a.

The appropriate value of D in the cleft is not known so we shall use three values of D which probably cover the range of possible values. In free solution, measurements of D vary between 5 and 7 $\times$ 10^{-6} cm^2/sec (Wang, 1953; Hodgkin & Keynes, 1957; Kushmerick & Podolsky, 1969; Nasi & Tillotson, 1985). The effective D in the cleft is almost certainly lower than this as a result of the obstruction to movement by the feet of the SR and other cytoplasmic inclusions. The lowest experimental value that we have found in the literature is 1.4×10^{-7} cm^2/sec (Hodgkin & Keynes, 1957; Kushmerick & Podolsky, 1969; Nasi & Tillotson, 1985). We shall do the calculation here, and the subsequent computations below, for the three values of $D = 5 \times 10^{-6}$, 1×10^{-6}, and 2×10^{-7} cm^2/sec. Substituting in Eq. (7), we find that $c_m = 0.29$, 1.45 and 7.25 mM for the three values of D and the above values for I and h.

Thus, the mean steady-state Ca concentration, c_m, in the cleft is increased from micromolar levels to millimolar. For the two lower values of D, it is in the range where significant binding by the low-affinity sites ($K_d = 1.1$ mM) would occur. The high-affinity sites would be totally saturated. Note that increasing the boundary condition at $r = a$ from 10^{-4} mM to a value between 10^{-4} and 5×10^{-3} mM would affect c_m only at the third decimal place. We need not, therefore, be concerned about our lack of knowledge about its true value or its time dependence.

Transient Problem, No Binding Sites

We now consider the time-dependent problem, in order to determine the time required to reach the steady state (if, indeed, the steady state can be reached in less than the 20-msec release period), and also the time beyond the 20-msec duration of the SR release, during which the elevated concentrations are maintained. Initially, we solve the problem in the absence of binding sites, partly because we are able to get an analytic solution only in this special case but also as a basis for comparison with our results below which determine the effect of the addition of sarcolemmal binding sites.

Considering conservation of Ca ions within the infinitesimal volume element between radial distance r and $r + dr$ during the time interval between t and $t + dt$, we obtain

$$[2\pi(r + dr)hJ(r + dr, t) - 2\pi rhJ(r, t)]dt = [c(r, t) - c(r, t + dt) + sdt]2\pi rhdr. \tag{8}$$

Taking the limit as dr and $dt \to 0$, and using Eq. (1) for s, Eq. (8) becomes

$$(1/r)\partial(rJ)/\partial r = -\partial c/\partial t + I/\pi a^2 h. \tag{9}$$

The left-hand side of Eq. (9) is the divergence of J in cylindrical coordinates with no z or θ dependence.

Using Eq. (3) to eliminate J, we obtain the diffusion equation

$$(D/r)\partial(r\partial c/\partial r)/\partial r = \partial c/\partial t - I/\pi a^2 h. \tag{10a}$$

This equation must be solved subject to the initial condition

$$c(r, 0) = c_0 \tag{10b}$$

that initially, at $t = 0$, the interior of the cleft is equilibrated with the intracellular medium and the boundary condition

$$c(a, t) = c_0 \tag{10c}$$

that for all time the outer cylindrical boundary $r = a$ of the cleft is maintained at the intracellular value c_0 (assumed constant).

The solution to the initial/boundary-value problem of Eqs. (10a–c) is (*see* Appendix A)

$$c(r, t) = c_0 + \frac{I}{4\pi Dh}\left[\left(1 - \frac{r^2}{a^2}\right) - 8\sum_{n=1}^{\infty} \exp(-j_{0,n}^2 Dt/a^2)\frac{J_0(j_{0,n}r/a)}{j_{0,n}^3 J_1(j_{0,n})}\right] \tag{11}$$

where J_0 and J_1 are the zero- and first-order Bessel functions of the first kind and $j_{0,n}$ is the n^{th} root of the equation

$$J_0(j_{0,n}) = 0 \tag{12}$$

which are tabulated (Abramowitz & Stegun, 1964, p. 409, Table 9.5). The first two values are $j_{0,1} = 2.4048\ldots$ and $j_{0,2} = 5.5201\ldots$ The first two terms in Eq. (11) are the steady-state solution of Eq. (6) and the third term, the infinite sum, is a sum of exponentials that decay to zero as $t \to \infty$. For sufficiently large t ($t \gg a^2/j_{0,1}^2 D$) the $n = 1$ term dominates and the concentration approaches the steady-state values (0.29, 1.45 and 7.25 mM) with time constants

$$\tau = a^2/j_{0,1}^2 D \tag{13}$$

which equal 0.064, 0.32 and 1.6 msec for $D = 5 \times 10^{-6}$, 1×10^{-6} and 2×10^{-7} cm^2/sec, respectively.

Note that when $t = 0$, the square-bracketed term in Eq. (11) is zero so that the initial condition is satisfied. This implies that $1 - r^2/a^2 = 8\sum_{n=1}^{\infty} j_{0,n}^{-3} J_0(j_{0,n}r/a)/J_1(j_{0,n})$. Using the known integral (Abramowitz & Stegun, 1964, p. 361, formula 9.1.30) $\int rJ_0(\alpha r)dr = J_1(\alpha r)/\alpha$ and averaging over the volume of the cleft, as in Eq. (7), the mean concentration is found to be

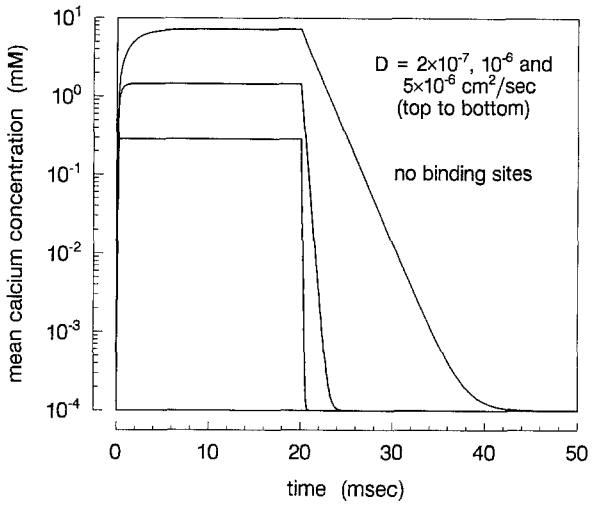

Fig. 2. Mean calcium concentration *versus* time in the absence of binding sites. The calcium concentration, averaged over the volume of the restricted space, is plotted as a function of time for three values of the diffusion coefficient, D. Results are from Eq. (14) for $0 \le t \le 20$ msec and from Eq. (17) for 20 msec $\le t \le 500$ msec.

$$c_m(t) = c_0 + (I/8\pi Dh) \times \left[1 - 32\sum_{n=1}^{\infty} j_{0,n}^{-4} \exp(-j_{0,n}^2 Dt/a^2)\right]. \tag{14}$$

Note that the square-bracketed expression vanishing at $t = 0$ implies that $\sum_{n=1}^{\infty} j_{0,n}^{-4} = \frac{1}{32}$. Equation (14) is shown by the rising phase of the curves in Fig. 2 for the three values of D.

To solve the problem after the release is turned off, it is assumed that the initial condition (i.e., the condition at $t = t_0 = 20$ msec) is the steady-state distribution of Eq. (6) so that the initial/boundary-value problem is

$$(D/r)\partial(r\partial c/\partial r)/\partial r = \partial c/\partial t \tag{15a}$$

$$c(r, t_0) = c_0 + (I/4\pi Dh)(1 - r^2/a^2) \tag{15b}$$

$$c(a, t) = c_0. \tag{15c}$$

The solution is (*see* Appendix A).

$$c(r, t) = c_0 + \frac{2I}{\pi Dh}\sum_{n=1}^{\infty} \exp(-j_{n,0}^2 D(t - t_0)/a^2)\frac{J_0(j_{0,n}r/a)}{j_{0,n}^3 J_1(j_{0,n})} \tag{16}$$

and averaging over r,

$$c_m(t) = c_0 + (4I/\pi Dh) \sum_{n=1}^{\infty} j_{0,n}^{-4} \exp(-j_{0,n}^2 D(t - t_0)/a^2). \quad (17)$$

The falling phase of the curve in Fig. 2 is obtained from Eq. (17). Note that the sum in Eq. (17), the falling transient, is just the negative of the sum in Eq. (14), the rising transient. The shapes of the two transients appear to be different only because of the logarithmic scale in the figure.

The conclusion up to this point is that, for the case of no sarcolemmal calcium binding sites, we can expect calcium concentration at millimolar levels while the SR release is occurring. However, upon cessation of release, [Ca] falls below 1 μM in < 15 msec for the case of slowest diffusion and in < 3 msec for the case of moderately slowed diffusion (Fig. 2).

Transient Problems with Binding Sites

We now add the Ca binding sites on the sarcolemmal surface opposite the SR cistern. We find that the addition of these sites significantly slows the build-up and decay of [Ca] in the cleft. The previous paper (Post & Langer, 1992) demonstrated two classes of binding sites. The density of the binding sites is derived as follows: our previous studies in cultured rat myocardial cells (Langer & Nudd, 1983; Post et al., 1988; Post & Langer, 1992) indicated that 1 kg wet cells contained 7.5 g sarcolemmal protein and the low-affinity sarcolemmal sites have a capacity of 85 nmol/mg protein. This indicates 6.4×10^{-4} mol Ca bound to sarcolemmal sites/kg cells. Page (1978) measures 0.31 μm^2 sarcolemmal membrane per μm^3 cell volume. Calculation then indicates a density of Ca binding sites of $N_1 = 2 \times 10^{-10}$ mol/cm^2 if the binding sites were uniformly distributed on the surface of the inner sarcolemmal leaflet. The density of the high-affinity sites is ~8% of the density of the low-affinity sites (7 nmol/mg protein) and would therefore have a density of $N_2 = 1.6 \times 10^{-11}$ mol/cm^2 if distributed in the same way. The K_d value for these two classes are $K_1 = 1.1$ mM and $K_2 = 13$ μM, respectively. The number of moles of Ca bound, c_b mol/cm^2, is assumed to follow a Michaelis-Menten relationship

$$c_b = N_1/(1 + K_1/c) + N_2/(1 + K_2/c). \quad (18)$$

The diffusion problem can be treated as being dependent only on r and t. That is, we neglect the slight z-dependence which must occur if the binding sites are located on the $z = h$ surface, since there must be a gradient in the z-direction to support the Ca flux toward or away from the binding sites. This neglect is permissible because $a \gg h$. Thus, in the model, the Ca source term arising from the Ca bound at $z = h$ can be treated as if it were smeared out in the z-direction between $z = 0$ and $z = h$. The result is thus the same as if the sites were distributed uniformly over the volume. The contribution of the binding sites, $-\partial c_b/\partial t$ per unit surface area or $-1/h \cdot \partial c_b/\partial t$ per unit volume, can be simply added to $-\partial c/\partial t$ on the right-hand side of the conservation Eq. (8) or (9), so that we have

$$(1/r)\partial(rJ)/\partial r = -\partial c/\partial t - (1/h)\partial c_b/\partial t + I/\pi a^2 h \quad (19)$$

in place of Eq. (9).

Using Eqs. (3), (18) and (19), we obtain the diffusion equation with binding

$$\frac{D}{r}\frac{\partial}{\partial r}\left(r\frac{\partial c}{\partial r}\right) = \left[1 + \frac{N_1/K_1 h}{\left(1 + \frac{c}{K_1}\right)^2} + \frac{N_2/K_2 h}{\left(1 + \frac{c}{K_2}\right)^2}\right]\frac{\partial c}{\partial t} - \frac{I}{\pi a^2 h} \quad (20)$$

where I has the same value used above for $0 < t < 20$ msec and is zero for $t > 20$ msec. In general, I could be an arbitrary function of time, and later we will consider the case of a train of square pulses to represent a beating cell. Equation (20) is a nonlinear equation which cannot be solved in analytic form. When analyzing cases for which $c \ll K_1$ or K_2 for all r and t, Eq. (20) can be linearized and solved analytically (Bers & Peskoff, 1991), but in the present case this inequality is not satisfied. In Appendix B we describe the numerical method used to solve Eq. (20) using Eqs. (B6), (B7), (B8) and (B12).

Substituting the above values for the physical parameters, we have for the dimensionless quantities $B_1 = N_1/K_1 h = 180$ and $B_2 = N_2/K_2 h = 1{,}200$. Physically, B_1 and B_2 are the number of low- and high-affinity binding sites on a differential area, dA, divided by the number of Ca ions in the corresponding differential volume, $h\,dA$, at half-saturation, i.e., at [Ca] = K_1 and K_2, respectively.

Before doing the numerical computation, one can anticipate the qualitative effect of the nonlinear factor in square brackets multiplying $\partial c/\partial t$, which represents the effect of binding, and which distinguishes Eq. (20) from Eq. (10a). Its effect is to stretch the scale of the time variations. The effective "time

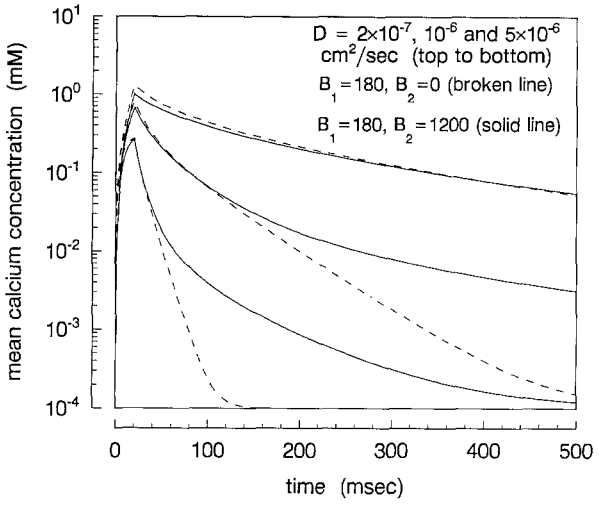

Fig. 3. Mean calcium concentration *versus* time with one and two classes of binding sites present. The calcium concentration, averaged over the volume of the restricted space, is plotted as a function of time for three values of diffusion coefficient, D. The broken curves are for low-affinity binding sites with $B_1 = N_1/K_1h = 180$. The solid curves are for the addition of high-affinity binding sites with $B_2 = N_2/K_2h = 1{,}200$. Results are from a finite-difference numerical solution of Eq. (20). Note the difference in time scale compared to Fig. 2.

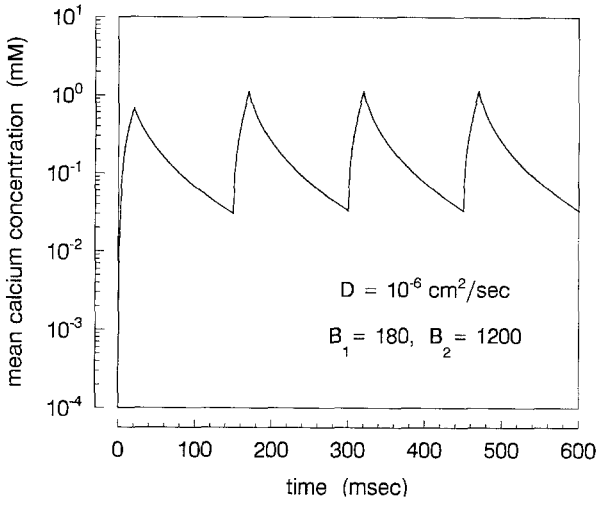

Fig. 4. Mean calcium concentration for repetitive Ca release from the SR, for the middle value of the diffusion coefficient, D, and both classes of binding sites. SR Ca is released as a train of pulses (400/min), each pulse identical to the pulse in Figs. 2 and 3.

constant" at time t will be of the order of τ in Eq. (13) multiplied by the square-bracketed expression in Eq. (20) evaluated at $c = c_m$.

As a function of c, the factor varies from 1 for $c \gg K_1$, to $\sim B_1$ for $c \sim K_1$, to $\sim (B_1 + B_2)$ for $c \leq K_2$. Solving for the value of c that makes the two Michaelis-Menten terms in Eq. (20) equal, yields

$$c = [(N_2/K_2)^{1/2} - (N_1/K_1)^{1/2}]/$$
$$[(N_1/K_1)^{1/2}/K_2 - (N_2/K_2)^{1/2}/K_1] = 21\ \mu\text{M} \qquad (21)$$

indicating that the effect of low- and high-affinity sites on the time constant are of equal magnitudes at $c = 21\ \mu$M.

The initial rate of decay of [Ca] following the 20-msec SR Ca release will depend on $c_m(t_0)$. For example, for $c_m(t_0) = K_1$, we expect initial slopes about $B_1/2$ times smaller in magnitude than in Fig. 2. The slopes will continuously decrease in magnitude as $c_m(t)$ decreases with increasing t. When $c_m = 21\ \mu$M, the slopes, according to Eq. (21), will be approximately $2B_1$ times smaller than the slopes at $c_m = 21\ \mu$M in Fig. 2. Finally, when $c_m \ll K_2$ they will be about $B_1 + B_2$ times smaller. Thus, we can expect a dramatic lengthening of the transient decay (roughly, between two and three orders of magnitude) caused by the presence of Ca binding sites. These expectations are confirmed by the numerical results which we now describe.

In Fig. 3 we show the result of numerical computation for $N_1/K_1h = 180$ and $N_2/K_2h = 1{,}200$ and the above values for I, a and h. The abscissa is the mean calcium concentration, c_m (on a logarithmic scale). It is obtained by computing c from the finite-difference approximation, Eq. (B13), and then averaging over volume, according to the average defined in Eq. (7), to obtain c_m. The three solid curves represent the time dependence of the [Ca] averaged over the volume of the cleft, for the same three values of the diffusion coefficient illustrated in Fig. 2. The dashed curves are the results if only the low-affinity sites are present (obtained by setting $N_2 = 0$ in Eqs. (20), (B6) and (B12)).

The $D = 5 \times 10^{-6}$ cm²/sec curves nearly reach the steady-state value shown in Fig. 2 within the 20-msec period of current flow. The dashed curve reaches a slightly higher peak value because, in the absence of high-affinity sites, less Ca is removed from the restricted space. The decay of the dashed curve is roughly 180 times slower and the decay of the solid curve is roughly 1,400 times slower than the corresponding curve where no binding sites are present (Fig. 2), confirming the qualitative expectation stated above. The $D = 10^{-6}$ and $D = 2 \times 10^{-7}$ cm²/sec curves again have slower time dependences than the $D = 5 \times 10^{-6}$ cm²/sec curve. None of the curves reach the steady-state concentrations of Fig. 2 because their effective time constants are greater than 20 msec, but they remain at high levels for a much longer period. For example, at $t = 100$ msec, the mean concentrations in the solid curves are about 0.004, 0.07 and 0.4 mM, for the three values of the diffusion coefficient.

Figure 4 shows the result of repetitive release of

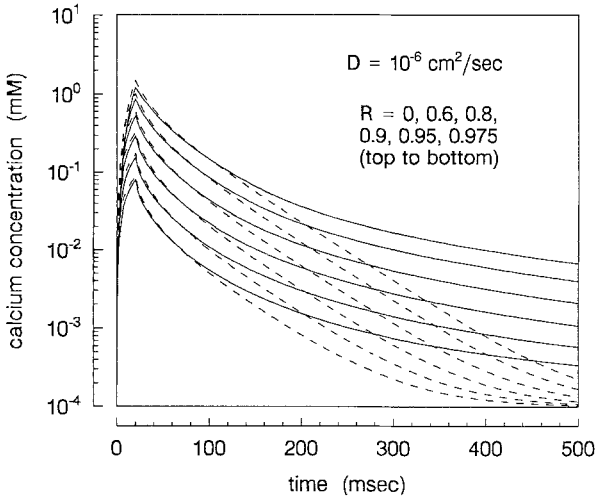

Fig. 5. Calcium concentration at six radial distances *versus* time. The same case as the middle, broken (low-affinity sites) and solid (low- and high-affinity sites) curves in Fig. 3 but showing the radial dependence of the calcium concentration.

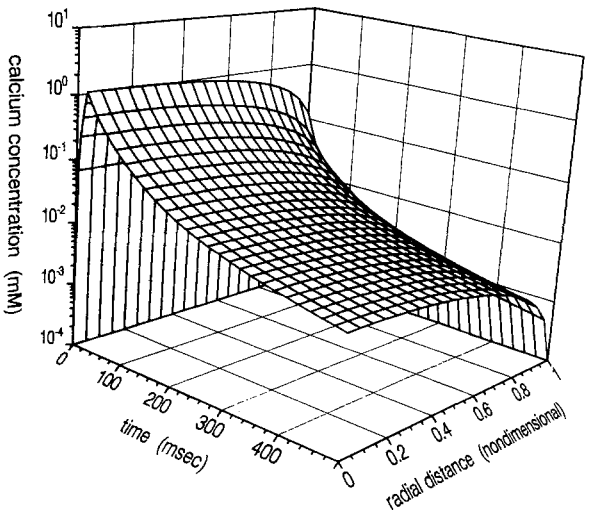

Fig. 6. Calcium concentration *versus* radial distance, $R = r/a$, and time. A three-dimensional plot of the solid curves in Fig. 5 (low- and high-affinity sites). The spatial dependence is shown at 4-msec increments for $0 \leq t \leq 20$ msec and at 20-msec increments for $20 \leq t \leq 500$ msec. The time dependence is shown at radial increments of 0.05.

the same amount of Ca from the SR, for four cardiac cycles at a heart rate of 400/min, typical for rat ventricle, for the middle value of $D = 10^{-6}$ cm^2/sec. To obtain this curve, for the source term on the right-hand side of Eqs. (20), (B6) and (B12) we take $I = 3.65 \times 10^{-17}$ mol/sec for $0 < t < 20$, $150 < t < 170$, $300 < t < 320$ and $450 < t < 470$ msec, and zero otherwise. The asymptotic shape of a single cycle is essentially attained in the second cycle. The mean concentration is above 0.1 mM for roughly half of each cycle.

Thus far we have illustrated the time dependence of the mean concentration, $c_m(t)$. To complete the picture, in Fig. 5 we show the time dependence of the concentration, $c(r, t)$, at selected radial distances, for the middle value of $D = 10^{-6}$ cm^2/sec and for $N_1/K_1h = 180$, $N_2/K_2h = 0$ (dashed), and $N_2/K_2h = 1{,}200$ (solid). The peak value of c at $r = 0$ is about double the peak value of c_m in Fig. 3. The spatial dependence of the concentration is relatively flat (on this logarithmic scale) for most of the distance out to $r = a$, with a fairly steep drop to $c_0 = 10^{-4}$ mM between the last curve at $r/a = 0.975$ and $r/a = 1$. Figure 6 is a three-dimensional view of the solid curves in Fig. 5.

Discussion

The most important consequence of the modeling of the Ca profile in the space (cleft) between the surface of the SR cistern and the inner sarcolemmal leaflet is the very large effect of the addition of calcium binding sites in the inner sarcolemmal leaflet on the mean (spatially averaged) concentration of Ca and its time-dependent changes.

In the case of moderate diffusion restriction ($D = 1 \times 10^{-6}$ cm^2/sec) the addition of only the low-affinity ($K_d = 1.1$ mM) sites at the density corresponding to uniform sarcolemmal distribution ($N_1/K_1h = 180$) reduces to about one-half, the maximum [Ca] that is attained in the cleft during SR release of Ca (Figs. 2 and 3). It is of greater significance, however, that the decay after cessation of release is greatly prolonged. [Ca] falls to 10% of its peak value within 2 msec in the absence of inner leaflet binding sites (Fig. 2). In their presence > 100 msec is required before [Ca] reaches 10% of its peak value (middle solid line in Fig. 3). The addition of the high-affinity sites ($K_d = 13$ μM) has little effect for the first 100 msec of decay, during which time mean [Ca] is > 0.1 mM, but considerable effect after [Ca] falls below ~13 μM (middle curves, Fig. 3).

We subsequently modeled the [Ca] profile in the cleft in the presence of the calcium binding sites for a rat ventricle stimulated at 400 excitations/min. Steady-state peak value of the spatially averaged [Ca] is achieved by the second beat at ~0.6 mM and does not fall below 30 μM during diastole. Obviously, at lower rates of stimulation [Ca] in the cleft approaches the diastolic level in the general cytoplasm.

The results just described refer to mean [Ca] within the cleft. Figure 5 presents the [Ca] at differ-

ent radial distances from the center to the periphery of the cleft. It is of interest that 100 msec after Ca release ceases the [Ca] is still > 30 μM at a point 80% of the distance to the outer boundary of the cleft. Between this radial distance and the boundary there is a decline in [Ca] to 1 μM. This is also shown in the three-dimensional plot (Fig. 6).

The documented presence of the sarcolemmal Ca binding sites in the cytoplasmic leaflet of the sarcolemma in the amounts measured in cultured cells (Post et al., 1988; Post & Langer, 1992) has significant physiological implications. Even with an amount of Ca released which will produce only 50% maximal ventricular force, [Ca] within the cleft rises to > 0.6 mM and remains > 20 μM for ~200 msec. If the sarcolemma at the cleft contains Na–Ca exchanger molecules, the profile of [Ca] in this region takes on particular significance. It has been shown recently that the Na—Ca exchanger molecules are concentrated in the part of the sarcolemma facing the cleft region (J.S. Frank, *personal communication*). The K_m(Ca) for the exchanger is in the range of 20 μM (Nicoll, Barrios & Philipson, 1991). This means that shortly after Ca release through the "feet" the exchanger is activated and remains > 50% activated for at least 200 msec after excitation. This indicates that net Ca efflux should be demonstrable during the course of the action potential and should be closely related to intracellular Ca release and its subsarcolemmal concentration. This is exactly what has been proposed by Egan et al. (1989) on the basis of measurements of Na—Ca exchange current in guinea-pig ventricular cells. The early efflux of Ca during the action potential was also demonstrated by Hilgemann (1986).

The inner leaflet anionic phospholipids may have an effect on the Na–Ca exchanger in addition to its regulation via [Ca] in the cleft. Philipson and Nishimoto (1984) have clearly demonstrated enhancement of exchanger activity (up to 300–400%) by the presence of anionic lipid components. Other transport systems such as the sarcolemmal Ca pump (Carafoli, 1990) and (Ca + Mg) ATPase (Verbist et al., 1991) are also significantly stimulated by anionic lipids in their environment.

As discussed above, the model emphasizes the important role of the sarcolemmal Ca binding sites in cellular Na–Ca exchange. It predicts the existence of a subsarcolemmal region where Ca concentration is significantly higher than in the cytosol. This calcium concentration is elevated to or above the K_m (20 μM) of the exchanger for a few hundred milliseconds following depolarization, allowing the exchanger to be activated to expel Ca from the cell in the amounts measured, over a period of ~200 msec. Diffusion in a restricted sarcolemmal space, even with a reduced diffusion coefficient, is not sufficient to produce the sustained elevation of [Ca] required (Fig. 2). To obtain this, our results indicate that it is necessary that the inner sarcolemmal surface facing the restricted space contain sites capable of binding Ca (Fig. 3). The experimentally demonstrated (Post et al., 1988) inner sarcolemmal leaflets phosphatidyl-serine, -inositol and -ethanolamine are more than sufficient to provide these sites.

Furthermore, the model also has significant implications for the process of Ca-induced Ca release. Fabiato (1983) proposed that the release is triggered by Ca entering the cell via Ca channels and calculated that the release is optimal in skinned cells from rat ventricle when the trigger pCa = 6.25 ([Ca] = 5.6×10^{-7}M) (Fabiato, 1983). Higher concentrations suppress release, with pCa = 5.25 ([Ca] = 5.6×10^{-6} M) almost totally suppressing it. Calcium entering the cell by means of transsarcolemmal fluxes therefore would diffuse to the "feet" and produce Ca-induced Ca release, which would result in a rapid increase of [Ca] in the cleft region (Fig. 3) and, therefore, in a rapid (< 2 msec) shutdown of the Ca-release channels. Unless the time constant for inactivation of release were much greater than that for activation, little Ca-induced Ca release would occur. Such a difference between time constants has, indeed, been proposed by Fabiato (1985).

References

Abramowitz, M., Stegun, I.A. (editors) 1964. Handbook of Mathematical Functions. National Bureau of Standards. Applied Mathematics Series 55, Washington, D.C.

Bers, D.M., Peskoff, A. 1991. Diffusion around a cardiac calcium channel and the role of surface bound calcium. *Biophys. J.* **59:**703–721

Carafoli, E. 1990. Sarcolemmal calcium pump. *In*: Calcium and the Heart. G.A. Langer, editor. pp. 109–126. Raven, New York

Crank, J. 1975. The Mathematics of Diffusion. (2nd ED.) Clarendon, Oxford

Egan, T.M., Noble, D., Noble, S.J., Powell, T., Spindler, A.J., Twist, V.W. 1989. Sodium-calcium exchange during the action potential in guinea-pig ventricular cells. *J. Physiol.* **411:**639–661

Fabiato, A. 1983. Calcium-induced release of calcium from the cardiac sarcoplasmic reticulum. *Am. J. Physiol.* **245:**C1–C14

Fabiato, A. 1985. Time and calcium dependence of activation and inactivation of calcium-induced release of calcium from the sarcoplasmic reticulum of a skinned canine cardiac Purkinje cell. *J. Gen. Physiol.* **85:**247–289

Feher, J.J., Fabiato, A. 1990. Cardiac sarcoplasmic reticulum: Calcium uptake and release. *In:* Calcium and the Heart. G.A. Langer, editor. pp. 199–268. Raven, New York

Hilgemann, D.W. 1986. Extracellular calcium transients at single excitations in rabbit atrium measured with tetramethylmurexide. *J. Gen. Physiol.* **87:**707–735

Hodgkin, A.L., Keynes, R.D. 1957. Movements of labelled calcium in squid giant axons. *J. Physiol.* **138:**253–281

Kushmerick, M.J., Podolsky, R.J. 1969. Ionic mobility in muscle cells. *Science* **166:**1297–1298

Langer, G.A., Nudd, L.M. 1983. Effects of cations, phospholipases and neuraminidase on calcium binding to "gas-dissected" membranes from cultured cardiac cells. *Circ. Res.* **53:**482–490

Nasi, E., Tillotson, D. 1985. The rate of diffusion of Ca^{2+} and Ba^{2+} in a nerve cell body. *Biophys. J.* **47:**735–738

Nicoll, D.A., Barrios, B.R., Philipson, K.D. 1991. Na^+–Ca^{2+} exchangers from rod outer segments and cardiac sarcolemma: Comparison of properties. *Am. J. Physiol.* **260:**C1212–C1216

Page, E. 1978. Quantitative ultrastructural analysis in cardiac membrane physiology. *Am. J. Physiol.* **4:**C147–C158

Philipson, K.D., Nishimoto, A.Y. 1984. Stimulation of Na–Ca exchange in cardiac sarcolemmal vesicles by phospholipase D. *J. Biol. Chem.* **259:**16–19

Post, J.A., Langer, G.A. 1992. Sarcolemmal calcium binding sites in heart: I. Molecular origin in "gas-dissected" sarcolemma. *J. Membrane Biol.* **129:**49–57

Post, J.A., Langer, G.A., Op den Kamp, J.A.F., Verkleij, A.J. 1988. Phospholipid asymmetry in cardiac sarcolemma. Analysis of intact cells and "gas-dissected" membranes. *Biochim. Biophys. Acta* **943:**256–266

Verbist, J., Gadella, T.W.J., Raeymaekers, L., Wuytack, F., Wirtz, K.W.A., Casteels, R. 1991. Phosphoinositide-protein interactions of the plasma membrane Ca^{2+} transport ATPase as revealed by fluorescence energy transfer. *Biochim. Biophys. Acta* **1063:**1–6

Wagenknecht, T., Grassucci, R., Frank, J., Saito, A., Inui, M., Fleischer, S. 1989. Three-dimensional architecture of the calcium channel/foot structure of sarcoplasmic reticulum. *Nature* **338:**167–170

Wang, J.H. 1953. Tracer-diffusion in liquids. IV. Self-diffusion of calcium ion and chloride ion in aqueous calcium chloride solutions. *J. Am. Chem. Soc.* **75:**1769–1770

Received 31 October 1991

Appendix A

The initial/boundary-value problem of Eqs. (10a–c) can be transformed to a homogeneous problem by defining the new variable

$$u(r, t) = c(r, t) - c_0 - \frac{I}{4\pi Dh}\left(1 - \frac{r^2}{a^2}\right) \tag{A1}$$

which is the concentration c minus its steady-state ($t \to \infty$) limit. Substituting Eq. (A1) in Eqs. (10a–c) yields

$$\frac{D}{r}\frac{\partial}{\partial r}\left(r\frac{\partial u}{\partial r}\right) = \frac{\partial u}{\partial t}$$

$$u(a, t) = 0 \tag{A2}$$

$$u(r, 0) = -\frac{I}{4\pi Dh}\left(1 - \frac{r^2}{a^2}\right).$$

The solution to this problem may be found by the method of separation of variables to be (Crank, 1975, p. 73, Eq. 5.18)

$$u(r, t) = \frac{2}{a^2}\sum_{n=1}^{\infty} \exp(-j_{0,n}^2 Dt/a^2)\frac{J_0(j_{0,n}r/a)}{J_1^2(j_{0,n})} \times \int_0^a ru(r, 0)J_0(j_{0,n}r/a)dr. \tag{A3}$$

J_0 and J_1 are the zero- and first-order Bessel functions of the first kind and $j_{0,n}$ is the n^{th} root of

$$J_0(j_{0,n}) = 0 \tag{A4}$$

which is tabulated (Abramowitz & Stegun, 1964, p. 406, Table 9.5). The integral in Eq. (A3) can be evaluated for the $u(r, 0)$ of Eq. (A2). Letting $R = r/a$ and, deleting the subscripts temporarily, letting $j_{0,n} = j$, yields

$$\frac{1}{a^2}\int_0^a r\left(1 - \frac{r^2}{a^2}\right)J_0\left(\frac{jr}{a}\right)dr = \int_0^1 (R - R^3)J_0(jR)dR. \tag{A5}$$

With the help of the derivative formulas for Bessel functions (Abramowitz & Stegun, 1964, p. 361, formula 9.1.30)

$$\frac{d}{dR}(RJ_1(jR)) = jRJ_0(jR) \tag{A6}$$

$$\frac{d}{dR}(J_0(jR)) = -jJ_1(jR) \tag{A7}$$

and integration by parts, the integral in Eq. (A5) can be evaluated

$$\int_0^1 RJ_0(jR)dR = \frac{J_1(j)}{j} \tag{A8}$$

$$\begin{aligned}\int_0^1 R^3J_0(jR)dR &= \int_0^1 R^2\left[\frac{1}{j}\frac{d}{dR}RJ_1(jR)\right]dR \\ &= \frac{R^3J_1(jR)}{j}\Bigg|_0^1 - \frac{2}{j}\int_0^1 R^2J_1(jR)dR \\ &= \frac{J_1(j)}{j} - \frac{2}{j}\int_0^1 R^2\left[-\frac{1}{j}\frac{d}{dR}J_0(jR)\right]dR \\ &= \frac{J_1(j)}{j} + \frac{2}{j^2}\left[R^2J_0(jR)\Big|_0^1 - 2\int_0^1 RJ_0(jR)dR\right] \\ &= \left[\frac{1}{j} - \frac{4}{j^3}\right]J_1(j)\end{aligned} \tag{A9}$$

where we used $J_0(j) = 0$ to get the last equality. Combining Eqs. (A8) and (A9),

$$\int_0^1 (R - R^3)J_0(jR)dR = \frac{4J_1(j)}{j^3} \tag{A10}$$

and Eq. (A3) becomes

$$u(r, t) = -\frac{2I}{\pi Dh}\sum_{n=1}^{\infty}\exp(-j_{0,n}^2 Dt/a^2)\frac{J_0(j_{0,n}r/a)}{j_{0,n}^2 J_1(j_{0,n})}. \tag{A11}$$

Substituting Eq. (A11) in Eq. (A1) yields Eq. (11). Substituting Eq. (11) in Eq. (7), using the integral in Eq. (A8), yields the mean concentration, c_m, of Eq. (14).

Letting $v(r, t) = c(r, t) - c_0$ in Eqs. (15a–c), yields

$$\frac{D}{r}\frac{\partial}{\partial r}\left(r\frac{\partial v}{\partial r}\right) = \frac{\partial v}{\partial t}$$

$$v(a, t) = 0$$

$$v(r, t_0) = \frac{I}{4\pi Dh}\left(1 - \frac{r^2}{a^2}\right). \tag{A12}$$

Equation (A12) is identical to Eq. (A2) except for a minus sign and the replacement of $t = 0$ by $t = t_0$ in the initial condition. The solution for $c(r, t)$ and $c_m(t)$ are thus as given in Eqs. (16) and (17).

Appendix B

Equation (20) was solved numerically by finite-difference approximation of the partial differential equation. Introducing the following variables and parameters:

$$R = r/a$$
$$T = Dt/a^2$$
$$B_1 = N_1/K_1 h$$
$$B_2 = N_2/K_2 h$$
$$S = (a^2/D)s = I/\pi Dh \tag{B1}$$

Eq. (20) becomes

$$\frac{1}{R}\frac{\partial}{\partial R}\left(R\frac{\partial c}{\partial R}\right) = \left[1 + \frac{B_1}{\left(1 + \frac{c}{K_1}\right)^2} + \frac{B_2}{\left(1 + \frac{c}{K_2}\right)^2}\right]\frac{\partial c}{\partial T} - S. \tag{B2}$$

The discrete variables are defined by

$$R_i = i\Delta R;\ i = 0, 1, 2, \ldots, L;\ \Delta R = 1/L$$
$$T_n = n\Delta T;\ n = 0, 1, 2, \ldots, M$$
$$c_i^n = c(aR_i, a^2T_n/D). \tag{B3}$$

The spatial derivative is replaced by

$$\frac{1}{R}\frac{\partial}{\partial R}\left(R\frac{\partial c}{\partial R}\right) = \frac{\partial^2 c}{\partial R^2} + \frac{1}{R}\frac{\partial c}{\partial R} \to \frac{c_{i+1}^n - 2c_i^n + c_{i-1}^n}{(\Delta R)^2} + \frac{1}{i\Delta R}\cdot\frac{c_{i+1}^n - c_{i-1}^n}{2\Delta R} \tag{B4}$$

and the time derivative by

$$\frac{\partial c}{\partial T} \to \frac{c_i^{n+1} - c_i^n}{\Delta T}. \tag{B5}$$

Substituting Eqs. (B3)–(B5) in (B2) and solving for c_i^{n+1}, the finite-different equation approximating Eq. (B2) is

$$c_i^{n+1} = c_i^n + \frac{[\Delta T/(\Delta R)^2]\left[c_{i+1}^n\left(1 + \frac{1}{2i}\right) - 2c_i^n + c_{i-1}^n\left(1 - \frac{1}{2i}\right)\right] + S\Delta T}{1 + \frac{B_1}{\left(1 + \frac{c_i^n}{K_1}\right)^2} + \frac{B_2}{\left(1 + \frac{c_i^n}{K_2}\right)^2}} \tag{B6}$$

for $i = 1, 2, 3, \ldots, L - 1$. The point $i = 0$ is treated separately below.

The initial condition of Eq. (10b) becomes

$$c_i^0 = c_0 \tag{B7}$$

and the boundary condition of Eq. (10c) becomes

$$c_L^n = c_0. \tag{B8}$$

By symmetry,

$$\partial c/\partial R = 0 \quad \text{at } R = 0. \tag{B9}$$

Using L'Hospital's rule to evaluate $(\partial c/\partial R)/R$ at $R = 0$,

$$\frac{\partial^2 c}{\partial R^2} + \frac{1}{R}\frac{\partial c}{\partial R} = 2\frac{\partial^2 c}{\partial R^2} \quad \text{at } R = 0 \tag{B10}$$

and placing an extra point at $i = -1$ and requiring $c_{-1}^n = c_1^n$ by symmetry, the difference approximation at $R = 0$ is

$$\frac{\partial^2 c}{\partial R^2} + \frac{1}{R}\frac{\partial c}{\partial R} \to \frac{2(c_1^n - 2c_0^n + c_{-1}^n)}{(\Delta R)^2} = \frac{4(c_1^n - c_0^n)}{(\Delta R)^2}. \tag{B11}$$

Substituting in Eq. (B2),

$$c_0^{n+1} = c_0^n + \frac{[4\Delta T/(\Delta R)^2][c_1^n - c_0^n] + S\Delta T}{1 + \frac{B_1}{\left(1 + \frac{c_0^n}{K_1}\right)^2} + \frac{B_2}{\left(1 + \frac{c_0^n}{K_2}\right)^2}}. \tag{B12}$$

The computation is done by starting with the initial condition c_1^0 of Eq. (B7) and then computing $c_i^1, c_i^2, \ldots, c_i^M$ successively, using Eq. (B12) for c_0^n and Eq. (B6) for c_i^n, $i = 1, 2, \ldots, L - 1$, and the boundary condition of Eq. (B8) for c_L^n (which appears in the equation for c_{L-1}^n).

In the computation, $\Delta R = 1/40$ ($L = 40$) and ΔT satisfied

$$\frac{\Delta T/(\Delta R)^2}{1 + B_1/(1 + c_0^n/K_1)^2 + B_2/(1 + c_0^n/K_2)^2} \leq 0.1 \tag{B13}$$

to avoid instability of the difference equation. Usually, the equality in Eq. (B13) was used. However, when c_0^n is small this leads to a ΔT that can be too large to follow the time dependence of c. When Eq. (B13) yielded a $\Delta T > 0.1\ D/a^2$, we took $\Delta T = 0.1\ D/a^2$.

To compute the mean concentration defined in Eq. (7), we used the trapezoidal rule

$$\frac{2}{a^2}\int_0^a rc(r, t)dr = 2\int_0^1 Rc(aR, a^2T/D)dR \rightarrow$$
$$\left[2\sum_{i=1}^{L-1}(ic_i^n) + Lc_L^n\right]\cdot(\Delta R)^2. \tag{B14}$$